Titanium Dioxide Nanoparticles Disturb the Fibronectin-Mediated Adhesion and Spreading of Pre-osteoblastic Cells

ARTICLE *in* LANGMUIR · AUGUST 2012

Impact Factor: 4.46 · DOI: 10.1021/la302219v · Source: PubMed

Langmuir

Article

pubs.acs.org/Langmuir

Titanium Dioxide Nanoparticles Disturb the Fibronectin-Mediated Adhesion and Spreading of Pre-osteoblastic Cells

Marie-Charlotte Bernier,[†,‡] Marie Besse,[†,‡,§] Muriel Vayssade,[‡] Sandrine Morandat,[§] and Karim El Kirat*[,‡]

[‡]Laboratoire de Biomécanique et Bioingénierie, Centre National de la Recherche Scientifique (CNRS) Unité Mixte de Recherche (UMR) 7338, and [§]Laboratoire de Génie Enzymatique et Cellulaire, Centre National de la Recherche Scientifique (CNRS) Unité Mixte de Recherche (UMR) 6022, Université de Technologie de Compiègne (UTC), BP 20529, 60205 Compiègne Cedex, France

Supporting Information

ABSTRACT: In the context of rapid development of nanoparticles (NPs) for industrial applications, the question of their toxicity and biological effects must be considered. In this work, we have assessed the influence of titanium dioxide NPs on the adhesion and spreading of MC-3T3 pre-osteoblasts by using a cell subclone that does not produce its own extracellular matrix. Petri dishes were coated with the important adhesion protein fibronectin (Fn). By incubating these Fn-coated surfaces with different amounts of TiO_2 NPs, we have shown that the adhesion of pre-osteoblasts is disturbed, with an important decrease in the number of adherent cells (from 40 to 75% depending upon the concentration and type of NPs). Petri-dish surfaces were analyzed with environmental scanning electron microscopy (ESEM), with images showing that TiO_2 NP aggregates are bound to the layer of adsorbed Fn molecules. The cells cultured on these Fn/NP surfaces adopted an irregular shape and an aberrant organization of actin cytoskeleton, as revealed by fluorescence microscopy. Most importantly, these results, taken together, have revealed that the actin cytoskeleton forms abnormal aggregates, even on top of the nucleus, that coincide with the presence of large aggregates of NPs on top of cells. On the basis of these observations, we propose that some Fn molecules are able to desorb from the Petri dish surface to coat TiO_2 NPs. Fn/NP complexes are not attached firmly enough on the surface to allow for normal cell adhesion/spreading and the development of tense actin fibers. These results stress the paramount need for the assessment of the toxicology of NPs, with special attention to their interactions with biomolecules.

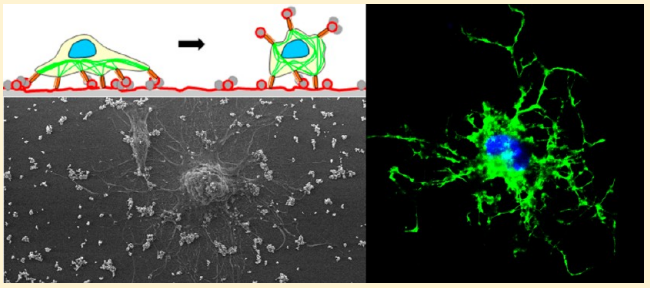

1. INTRODUCTION

Although nanoparticles (NPs) are promised a bright industrial future, their toxicology is still a matter of debate and little is known about their association with biomolecules. However, it is now clear that, when NPs are released in a biological environment, they can easily bind biomolecules, which may result in the acquisition of new properties. For example, if ligands from biological fluids adsorb on NPs, the resulting complexes could interact with specific receptors from the cell surface. Then, various cellular responses can be anticipated, but most importantly, the NPs could be abnormally hidden by adsorbed biomolecules, a situation that is reminiscent of a Trojan horse. As a consequence, NPs covered with biomolecules could be addressed to specific organs and cells, where they would accumulate and possibly express their toxicity. In fact, these hypotheses highlight the importance for toxicology to consider the association of NPs with biomolecules.

As described previously in the literature, NPs can become covered with proteins from biological fluids, leading to the formation of a protein corona.[1−3] As a result, the authors who studied protein/NP associations have suggested that the ligand-mediated uptake by cells can be greatly affected.[2,4] In recent years, several groups have studied the interactions between NPs and seric proteins.[5−10] For example, NPs are able to associate with seric proteins, such as the transforming growth factor TGF-β,[11] cytokines,[12] and albumin.[13] The biological functions of these seric proteins are quite different; therefore, their complexes formed with NPs may induce different biological responses. As a consequence, the protein corona defines the biological identity of NPs because this proteic coating is what the cells really "see".[14] The adsorption of proteins could then transform nontoxic NPs into toxic NPs and vice versa, by modulating their biological route, fate, and accumulation.[15] It is important to note that the protein corona is not frozen; it evolves with time and with the composition of biological fluids.[16,17] In biological fluids, the protein corona is initially formed around NPs by the adsorption of highly concentrated proteins (e.g., albumin is the most abundant plasma protein). Then, they could be replaced in the protein corona with less concentrated proteins having a higher association affinity for the surface of NPs.[8] Besides NPs, the competitive turnover of

Received: May 31, 2012
Revised: August 29, 2012
Published: August 30, 2012

proteins on surfaces is a well-known fact.[18,19] Given the numerous combinations of protein/NP associations, it is now clear that it will be very difficult to define the toxicology of nanosized materials completely.

The extensive use of titanium implants in dentistry and restorative surgery calls for special attention to their biological safety. This material has a good biocompatibility because of the 5−6 nm thick layer of TiO_2 that is spontaneously formed on its surface.[20−22] Such prostheses are generally prone to frictional wear, and the resulting debris can be as small as nano-objects.[23] These nano-debris may cause health problems either at the implant site or in distant organs.[24] Moreover, the use of NPs in the fabrication of biomaterials is currently proposed as an application to improve their mechanical/chemical resistance and/or biocompatibility.[25−27] Therefore, NPs can be generated at the surface of biomaterials on which cells are expected to attach and spread. This is particularly the case for the osseointegration procedure of bone prostheses; cells have to colonize and migrate in the implant for optimal efficacy. As suggested in the literature, adhesion, wear, and friction may play an important role in (re)modeling the bone−implant interface and the biological reaction to wear debris can be the induction of osteolysis.[28,29] The *in vitro* biological reaction of pre-osteoblasts to TiO_2 anatase NPs corroborates these assumptions; the secretion of the inflammation marker interleukin-6 by osteoblasts is significantly increased in the presence of NPs.[30]

In this work, we have assessed the cellular effect of the interaction between surfaces coated with fibronectin (Fn) and TiO_2 NPs. Fn is a high-molecular-weight glycoprotein (disulfide-linked dimer of approximately 440 kDa) having a modular structure. Fn is present in plasma and extracellular matrices, where it plays a crucial role in many processes, including cell adhesion, morphology, migration, thrombosis, and embryonic differentiation.[21] Fn is recognized by membrane-spanning integrin receptors from the cell surface to ensure cell adhesion.[31] Other modules on the structure of Fn contribute to the organization of the extracellular matrix by binding specific biomolecules: collagen, fibrin, and heparan sulfate proteoglycans.[32] Our results revealed that Fn significantly increases the binding of NPs to solid surfaces, which, in turn, disturbs the adhesion and spreading of MC-3T3 pre-osteoblast cells. Interestingly, the actin cytoskeleton presents an aggregated and ramified structure even on top of cells, suggesting that Fn/NP complexes bound to the surface are recognized by integrin receptors of cells but could not serve as firm adhesion points to spread cells. It is also important to note that, under the conditions chosen for cytotoxicity assessment, i.e., by adding NPs on already spread cells, the morphology of MC-3T3 was not modified.[30] Thus, it reinforces the notion that the effects of NPs on cell shape are due to their interaction with Fn molecules.

2. EXPERIMENTAL SECTION

2.1. Materials. Commercially available TiO_2 NP powders from Sigma-Aldrich (Saint-Quentin Fallavier, France) were anatase form (AN-NPs, titanium oxide anatase nanopowder, average primary particle diameter of <25 nm with a specific surface area of 200−220 m^2/g) and rutile form coated with silicon dioxide (RU-NPs, average particle size of 10 × 40 nm with a specific surface area of 130−190 m^2/g). Human serum albumin (HSA), Triton X-100, and 4′,6′-diamidino-2-phenylindole (DAPI) were also from Sigma-Aldrich and were used without further purification. Fn was from Roche Diagnostic (Mannhein, Germany). Minimum essential medium (MEM)α, L-glutamine, fetal bovine serum (FBS), penicillin, streptomycin, and trypsin−ethylenediaminetetraacetic acid (EDTA) (0.25%) were from Invitrogen (Cergy Pontoise, France). Phalloïdin-X5-fluoprobes 505 was purchased from Interchim (Montluçon, France). Mowiol mounting medium for fluorescence microscopy was from Calbiochem (Meudon, France). All other chemicals, including buffers and salts, were from Merck (Darmstadt, Germany) and were of analytical grade.

2.2. Preparation and Characterization of TiO_2 NP Suspensions. AN-NPs and RU-NPs were chosen because they are representative of those used in manufactured products (for example, anatase TiO_2 is employed in paints because of its photocatalytic properties, and silica-coated rutile is used in cosmetics). These NPs were analyzed by transmission electron microscopy (TEM), and the images (data not shown) provided results that are similar to those described previously by other authors for the same commercial references.[33,34] NPs were sterilized by heating to 120 °C for 20 min and then dispersed in a phosphate-buffered saline (PBS) in sealed sterile tubes to prepare two stock solutions, at 2500 or 25 000 μg/mL, depending upon the final concentrations to be used. To avoid aggregation, the suspensions were sonicated for 30 min (170 W, 35 kHz, Transsonic 275 T460, Prolabo). Particles were suspended and sonicated just before use.

TiO_2 NPs were characterized (size and aggregation) in PBS and with Fn using dynamic light scattering (DLS; Nanosizer, Malvern Instruments, Ltd.). DLS data were treated with the software supplied by Malvern, DTS Nano, version 5.03. The mean hydrodynamic diameter was calculated from the autocorrelation function of light intensity scattered from the NPs on the basis of at least three independent measurements.

2.3. Fn Coating and Incubation with NPs. Human plasma Fn (1 mg/mL) was diluted in PBS buffer to a final concentration of 50 μg/mL, which was high enough to saturate the surface of Petri dishes with Fn.[35] The adsorptions were performed by incubating tissue culture polystyrene Petri dishes (Nunclon, Dominique Dutscher, France) with Fn solutions at 37 °C for 45 min. The surfaces were then washed 3 times for 10 min in PBS at room temperature. NPs were incubated with surfaces at two concentrations (40 and 400 μg/mL) for 60 min at 37 °C. Prior to cell seeding, surfaces were rinsed 3 times with PBS buffer.

2.4. Cell Culture and Cell Adhesion Studies. Pre-osteoblasts MC-3T3 E1 subclone 24 (ATCC, CRL-2593, LGC Promochem, France) were cultured in MEMα supplemented with 10% FBS, 1% L-glutamine, penicillin (100 units/mL), and streptomycin (100 units/mL). The subclone 24 of MC-3T3 pre-osteoblasts was chosen to study the influence of TiO_2 NPs on cell adhesion specifically because they are not able to produce their own extracellular matrix; therefore, they are forced to use the exogeneously added Fn. In culture conditions, cells were maintained at 37 °C in a humidified atmosphere containing 5% CO_2. For cell adhesion analyses, MC-3T3 pre-osteoblasts were seeded in serum-free medium on Fn-coated surfaces treated with NPs at 10^4 cells/cm^2 and incubated at 37 °C for 2 h. The supernatants were removed, and adherent cells were incubated with trypsin−EDTA (0.25%) for 4 min at 37 °C. The trypsin reaction was stopped by adding FBS, which inhibited the protease; the cells were then pelleted by centrifugation at 200*g* and finally collected and counted using a Malassez hemacytometer.

2.5. Surface Analysis. Petri-dish surfaces were investigated by environmental scanning electron microscopy (ESEM). In the case of bare surfaces or surfaces coated with Fn and NPs, the samples were rinsed once with PBS and once with ultrapure water to remove buffer salts and examined immediately by ESEM (FEG XL30, Philips). Concerning surfaces with cells, they were washed with PBS and then fixed with Rembaum buffer (15 mM phosphate buffer, 1 mM EDTA, 133 mM NaCl, 5 mM KCl, and 3% glutaraldehyde). The fixed samples were finally washed 3 times with ultrapure water immediately before examination by ESEM. ESEM images were analyzed using ImageJ software [National Institutes of Health (NIH), Bethesda, MD].

2.6. Confocal Fluorescence Microscopy. Fn-coated surfaces with cells were washed 3 times with PBS buffer, and cells were fixed by incubation in 4% *para*-formaldehyde at room temperature for 10 min

dx.doi.org/10.1021/la302219v | *Langmuir* 2012, 28, 13660−13667

and permeabilized with PBS containing 1% Triton X-100. Surfaces were then incubated with PBS containing Phalloïdin-X5-fluoprobes 505 (0.066 nmol/mL) and DAPI (1 μg/mL). Samples were then washed with PBS, mounted in mowiol, and examined under a confocal microscope (LSM 710, Zeiss, France). Confocal fluorescence images were analyzed using ImageJ software (NIH, Bethesda, MD). These analyses permitted to determine the area and perimeter of zones covered with the actin cytoskeleton to calculate the circularity C ($C = 4\pi A/P^2$; C varies from 0 to 1, with the value 1 corresponding to a circular shape). The circularity was determined on the outline of the actin network of single cells to compare the modifications induced by NPs.

2.7. Statistical Analysis. Data are expressed as the mean ± standard deviation. InStat3 software (GraphPad) was used to perform a Kruskal–Wallis test [non-parametric analysis of variation (ANOVA)], followed by a post-hoc Dunn test for comparison to controls.

3. RESULTS AND DISCUSSION

3.1. Characterization of TiO_2 NPs and Their Binding to Surfaces Coated with Fn. We have studied the ability of TiO_2 NPs to associate with Fn molecules adsorbed on a surface. We have chosen two types of commercially available TiO_2 NPs that are the most used in industrial applications: AN-NPs are used as photocatalysts (e.g., in paints),[36] and RU-NPs coated with inert silica are generally used in cosmetics [e.g., in sunscreens, the silica coating increases their dispersibility in aqueous solutions and avoids the production of reactive oxygen species because of ultraviolet (UV) photocatalysis of TiO_2 NPs, which prevents contact catalysis with the skin or organic compounds].[37,38] First, NPs were characterized in buffer solution with DLS. DLS measurements provided diameters of 456 ± 55 and 452 ± 21 nm for aggregates of AN-NPs and RU-NPs, respectively. These values are in the range of those reported previously.[7] By adding Fn at 50 μg/mL to NPs in solution, the diameter of AN-NPs was kept constant at 459 ± 107 nm and increased up to 1422 ± 112 nm for RU-NPs. This effect suggests that Fn molecules do not interact with AN-NPs in solution, while they agglomerate the aggregates of RU-NPs. In contrast, the protein HSA increased the diameter of AN-NPs and RU-NPs in solution: 624 ± 93 and 724 ± 48 nm, respectively. These results suggest that HSA agglomerates TiO_2 NPs in PBS.

The interaction of NPs with Fn pre-adsorbed on surfaces was analyzed with ESEM (Figures 1 and 2 for AN-NPs and RU-NPs, respectively). First, bare Petri dishes (i.e., without Fn) were incubated with NPs to verify their ability to interact with the solid support. After rinsing to remove excess NPs, ESEM images revealed the presence of NPs bound to surfaces (images A and B of Figures 1 and 2). In the case of AN-NPs, the surface was sparsely covered with some aggregates of NPs (images A and B of Figure 1; surface coverage with NPs of about 1.7 ± 0.5%). For RU-NPs, the Petri-dish surface was covered with aggregates but large areas were still not covered (images A and B of Figure 2; surface coverage with NPs of about 4.0 ± 0.7%). From these ESEM images, we have determined the diameter of NPs: 339 ± 127 and 304 ± 117 nm for AN-NPs and RU-NPs, respectively. Clearly, in comparison to the results obtained in solution, the size of aggregates decreased for both types of NPs when they were adsorbed on the bare surface. When the surfaces were coated with Fn before the incubation with NPs, the amount of NP aggregates found on the surface was greatly increased for both types of particles (images C and D of Figures 1 and 2). As seen in these images, AN-NPs were able to form a layer of large aggregates (450 ± 200 nm) bound to the surface (NP surface coverage of about 22.0 ± 2.7%). Concerning RU-

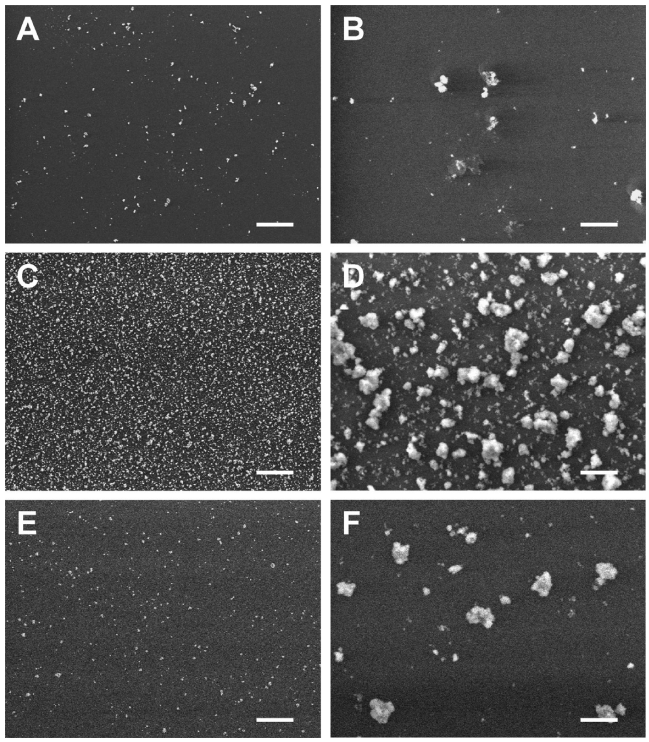

Figure 1. ESEM images of Petri-dish surfaces incubated with AN-NPs (400 μg/mL) (A and B) without Fn, (C and D) coated with Fn at 50 μg/mL, and (E and F) coated with HSA at 330 μg/mL. Scale bars are (A, C, and E) 20 μm and (B, D, and F) 2 μm.

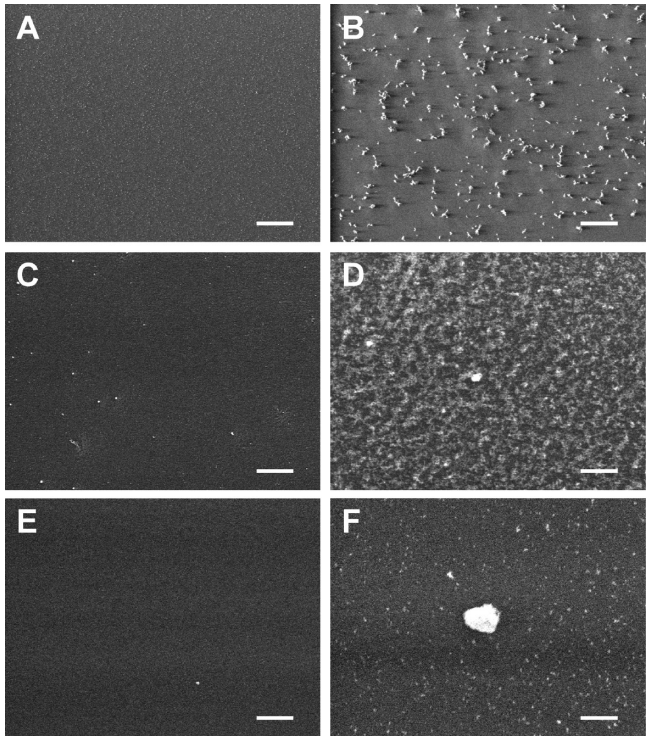

Figure 2. ESEM images of Petri-dish surfaces incubated with RU-NPs (400 μg/mL) (A and B) without Fn, (C and D) coated with Fn at 50 μg/mL, and (E and F) coated with HSA at 330 μg/mL. Scale bars are (A, C, and E) 20 μm and (B, D, and F) 2 μm.

dx.doi.org/10.1021/la302219v | Langmuir 2012, 28, 13660–13667

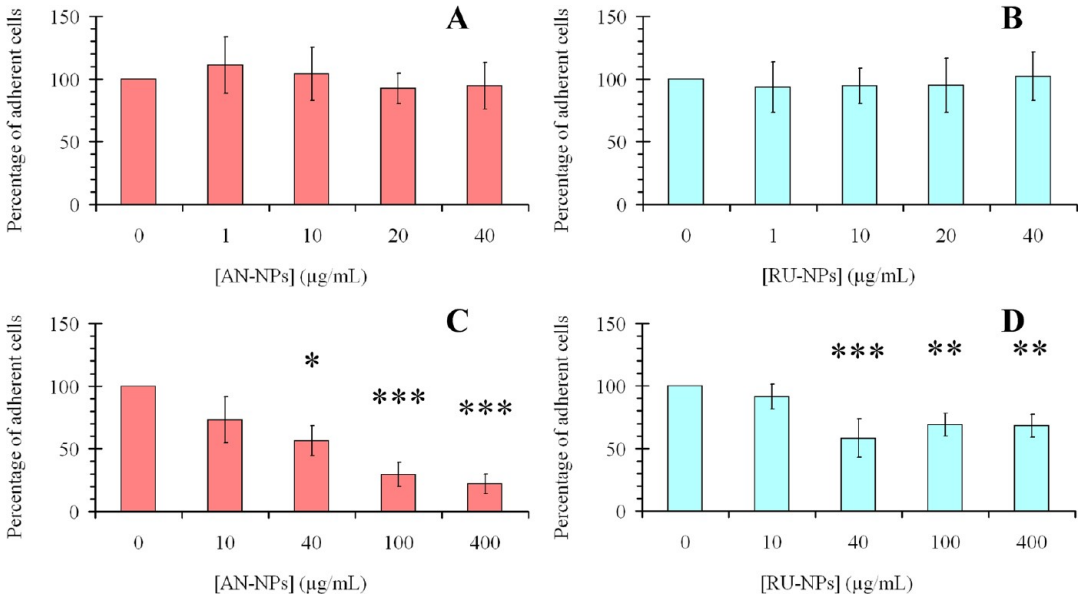

Figure 3. Influence of NPs on the adhesion of MC-3T3 cells to (A and B) bare or (C and D) Fn-coated surfaces treated with AN-NPs (red bars) or RU-NPs (blue bars). Results are the mean ± standard deviation of three separate experiments performed in triplicate. Asterisks indicate significant differences versus control cells (Dunn test): (*) $p < 0.05$, (**) $p < 0.01$, and (***) $p < 0.001$.

NPs, they formed a quasi-continuous layer on adsorbed Fn, indicating a dispersive effect. The crumbling of RU-NP aggregates on Fn-coated surfaces did not permit us to determine their size, but their surface coverage was found to be 35.0 ± 9.8%. These results on Fn-coated surfaces clearly differ from those obtained in solution with DLS. It shows the importance of studying the interactions of NPs with proteins in a context that is relevant to their biological function. Interestingly, the amount of NPs bound to surfaces precoated with HSA was very low, suggesting that the attachment of NPs to the surface depends upon the type of adsorbed proteins (images E and F of Figures 1 and 2; surface coverage of 4.1 ± 0.5%).

3.2. Influence of NPs on the Adhesion of Cells on Fn-Coated Surfaces. In these experiments, NPs were first incubated in Petri dishes either bare or coated with Fn. NPs that were not bound to the surface were removed by multiple rinses. Then, MC-3T3 cells were added in Petri dishes, and they were allowed to attach and spread on the surface for 2 h, the appropriate amount of time to gain information specifically about cell adhesion.[39−41] It is worth noting that after 2 h of culture in contact with adsorbed NPs, pre-osteoblasts revealed no toxicity or cell injury, as measured with the trypan blue assay (data not shown). Despite the use of Raman spectroscopy, it was difficult to quantify adsorbed NPs directly, but according to ESEM images (and surface coverages), this amount was quite low (Figures 1 and 2). Therefore, on the basis of the trypan blue assay and our previous work with MC-3T3 cells (TiO_2 NPs are cytotoxic at concentrations greater than 20 μg/mL), we can assume that the modifications observed here are not related to toxicity.[30] MC-3T3 pre-osteoblast cells were seeded in bare Petri dishes in the presence of different concentrations of NPs. After 2 h, we have counted the number of cells that were able to stay attached to the surface after multiple rinses (histograms A and B of Figure 3). As one can see in these histograms, the presence of NPs in the culture medium during the cell seeding has no influence on cell adhesion. Petri dishes coated with Fn were incubated with different concentrations of NPs. After rinses to remove free NPs, cells were left to attach on surfaces for 2 h. The results obtained under these conditions revealed that cell adhesion was greatly reduced (histograms C and D of Figure 3). In the case of AN-NPs, we found that the number of cells able to adhere to the surface decreased by approximately 75% with 400 μg/mL NPs. With RU-NPs adsorbed on Fn surfaces, we found that the adhesion of cells decreased by 40% at maximum. By considering ESEM images of NPs bound to Fn-coated surfaces, one can easily imagine that NPs can suppress the access to specific cell adhesion motifs (RGD consensus sequence) on Fn molecules. Such masking of specific portions of Fn molecules could then hinder their recognition by integrin receptors of osteoblasts. This hypothesis of molecular hindrance was further tested using antibodies that are specific for different regions of Fn molecules (against the entire Fn molecule or specific for the RGD consensus sequence). The results of enzyme-linked immunosorbent assays (ELISAs) indicated that there is no molecular obstacle in the access to specific regions of Fn molecules even when the concentration of NPs was high, independent of the type of TiO_2 NPs (see the Supporting Information).

3.3. Structure of Cells Cultured on Fn/NP Surfaces. The morphology of MC-3T3 cells cultured on Fn/NP surfaces was analyzed with ESEM (Figures 4 and 5 for AN-NPs and RU-NPs, respectively). As seen in these images, the morphology of cells was considerably altered by the presence of NPs bound to the surface. Indeed, as shown in images A and B of Figure 4, pre-osteoblasts cultured on surfaces coated with Fn were well-spread and the cell boundaries were well-identified (see white arrow in Figure 4A). In the presence of low amounts of TiO_2 AN-NPs bound to adsorbed Fn molecules, the morphology of cells was completely modified (images C and D of Figure 4). Indeed, the outline of the cell was much more irregular on culture surfaces presenting Fn/AN-NPs; thick filamentous extensions were formed (see white full line arrow in Figure 4D), and the surface of the cell body became irregular (see dotted arrow in Figure 4D). It is also important to note that the cells presented some NPs bound to

dx.doi.org/10.1021/la302219v | Langmuir 2012, 28, 13660−13667

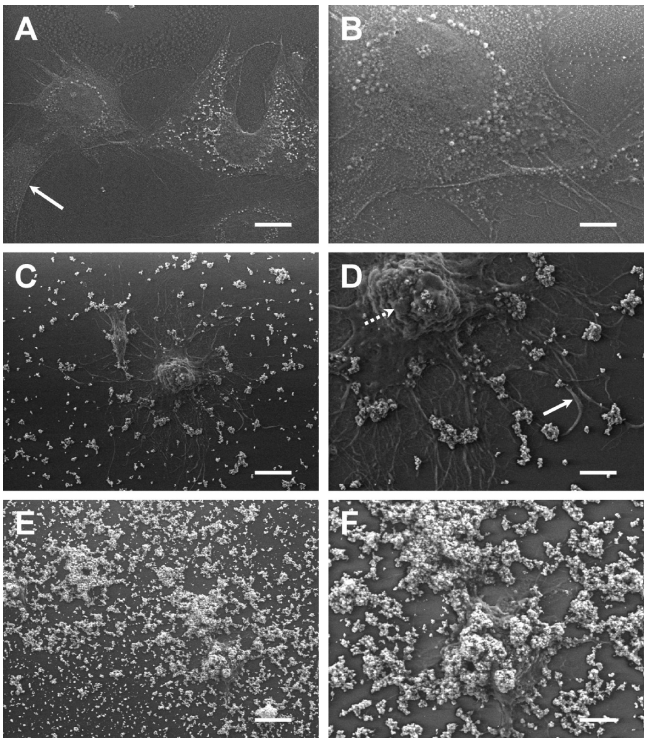

Figure 4. ESEM images of cells cultured on Fn-coated surfaces (A and B) without NPs or with AN-NPs at (C and D) 40 μg/mL and (E and F) 400 μg/mL. The surfaces were rinsed to remove free AN-NPs before cell seeding. The white arrows indicate thick filamentous structures (full line) and the irregular cell surface (dotted line). Scale bars are (A, C, and E) 20 μm and (B, D, and F) 2 μm.

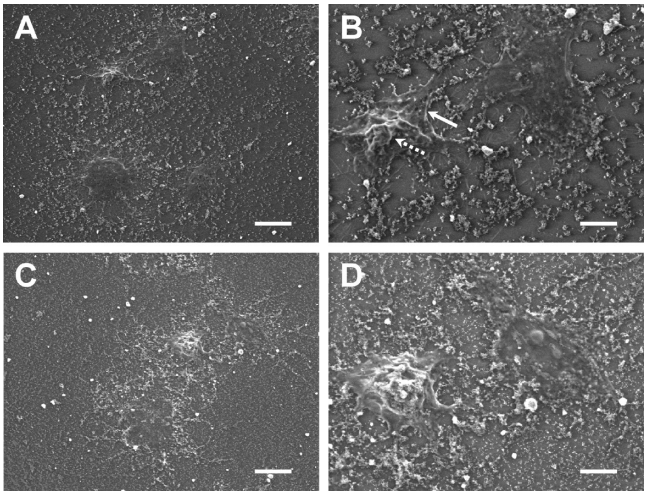

Figure 5. ESEM images of cells cultured on Fn-coated surfaces with RU-NPs at (A and B) 40 μg/mL and (C and D) 400 μg/mL. The surfaces were rinsed to remove free RU-NPs before cell seeding. The white arrows indicate thick filamentous structures (full line) and the irregular cell surface (dotted line). Scale bars are (A and C) 20 μm and (B and D) 2 μm.

their surface. With very high amounts of AN-NPs adsorbed on the Fn layer, the cells were completely covered with AN-NPs and were even less spread on the surface (images E and F of Figure 4). Interestingly, AN-NPs were redistributed on the surface during the incubation with cells (compare images E and F of Figure 4 to images C and D of Figure 1). These images prove the redistribution of AN-NPs and their accumulation at the surface of MC-3T3 cells. In the case of RU-NPs at a low concentration, the cells were modified very similarly to those treated with AN-NPs in terms of morphology (filamentous extensions, cell outline disturbed, and cell body roughening) (images A and B of Figure 5). Even if they could not be distinguished as easily as AN-NPs because they were dispersed by Fn as mentioned above, RU-NPs were also stuck to the cell surface. They are visible in images with high amounts of surface-bound RU-NPs (images C and D of Figure 5). In fact, the rough structure of the cell body and the presence of thick filaments at the boundary of cells suggest a disruption of the cytoskeleton structure.

We have checked the organization of the actin cytoskeleton of cells with specific fluorescent labeling and confocal imaging. As shown on images A and B of Figure 6, the actin cytoskeleton

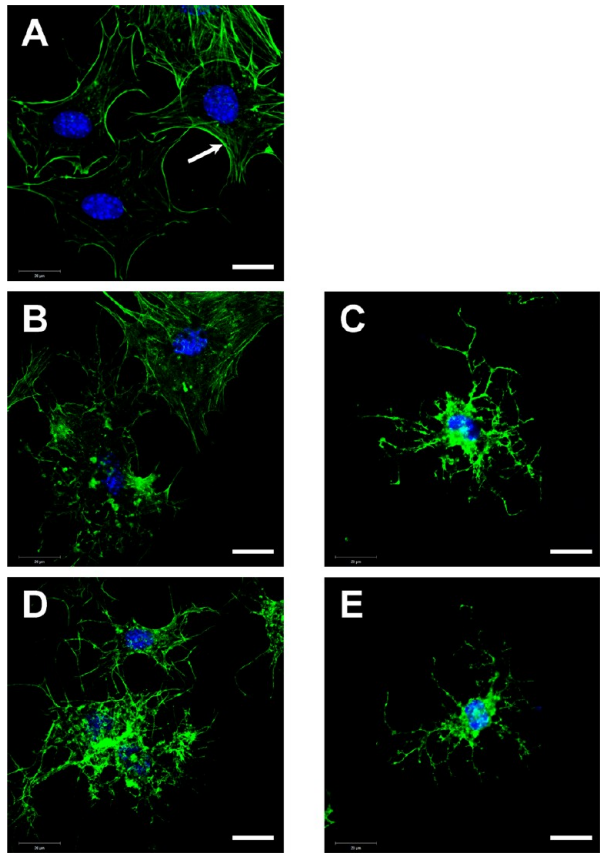

Figure 6. Fluorescent confocal microscopy images of cells cultured on Fn-coated surfaces (A) without NPs, with AN-NPs at (B) 40 μg/mL and (C) 400 μg/mL, or with RU-NPs at (D) 40 μg/mL and (E) 400 μg/mL. The surfaces were rinsed to remove free NPs before cell seeding. The nuclei were stained with DAPI (blue), and the actin cytoskeleton was revealed with fluorescent phalloidin (green). The white arrow indicates well-formed tense actin fibers. Scale bars are 20 μm.

of pre-osteoblasts spread on a surface coated with Fn presents a fine structure and well-identified tense actin filaments supporting the cell membrane (see white arrow in Figure 6A; actin network circularity is of about 0.250 $\pm$ 0.01). It is worth noting that no actin filaments could be found on top of the nucleus (colored in blue with DAPI staining). In the presence of NPs, the morphology of the actin network changed dramatically (images B–E of Figure 6). Indeed, the actin filaments formed aggregates in the cells, and in the case of a

dx.doi.org/10.1021/la302219v | *Langmuir* 2012, 28, 13660–13667

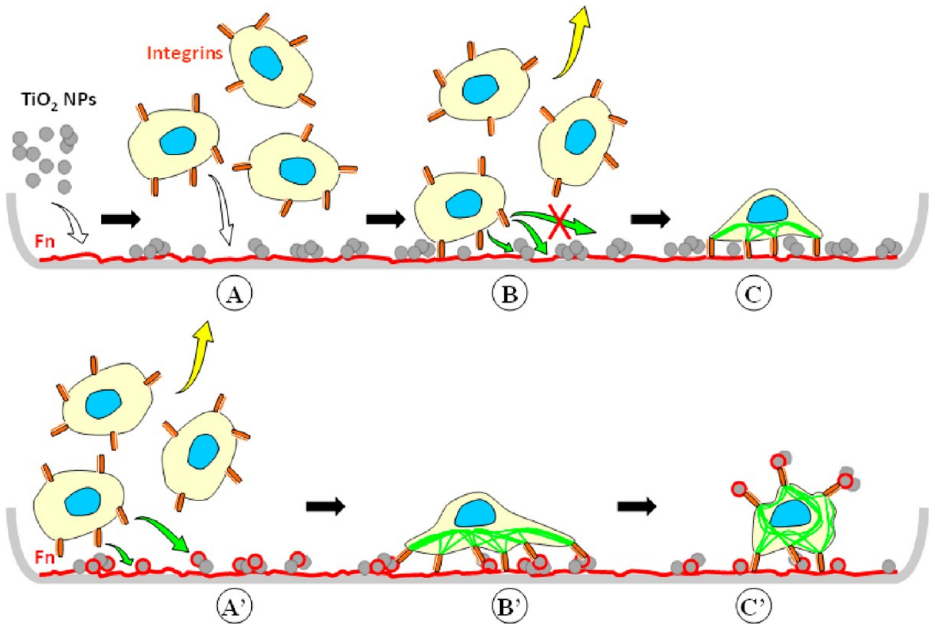

Figure 7. Mechanisms proposed to explain how NPs can disturb cell adhesion on Fn-coated surfaces. Fn (red) was first adsorbed on Petri dish surfaces. Surfaces were then treated with NPs (gray). After rinsing to remove free NPs, the cells were seeded (A and A′). By assuming that NPs do not interfere with the specific recognition between Fn and integrin molecules (as demonstrated with ELISAs), two hypotheses can be proposed. First, cells attached to the surface in areas where Fn molecules are accessible (B), and then they tried to spread on the surface. If NPs were tightly bound to the surface, they constitued a topography with physical obstacles to cell adhesion; therefore, cells attached and spread only moderately (C). During this step, the recognition of adsorbed Fn molecules by integrin receptors of cells provoked the development of the actin cytoskeleton (green). In the second hypothesis, Fn molecules were able to desorb from the surface to coat NP aggregates (A′). In fact, integrins of cells could bind Fn molecules on surfaces or on NPs (B′). If we consider that Fn/NP complexes are weakly bound to the surface, the cells could not us them to form tense actin fibers. When Fn/NPs detached from the surface, the relaxation of the traction force exerted by cells through the actin fibers may have produced the abnormal repartition of actin cytoarchitecture and the accumulation of NPs at the surface of cells (C′).

high concentration of NPs, the filaments were elongated, sometimes with a ramified structure (images C and E of Figure 6). Abnormal aggregates of actin were also visible on top of the cell nucleus, which is unsual for cells attached to surfaces. Moreover, the circularity C of the actin network of cells decreased dramatically. Indeed, at 40 μg/mL NPs, the circularity was reduced to 0.033 ± 0.002 and 0.018 ± 0.001 for AN-NPs and RU-NPs, respectively. These low values of C were confirmed at 400 μg/mL NPs: 0.074 ± 0.005 and 0.020 ± 0.001 for AN-NPs and RU-NPs, respectively.

The correct positioning and development of the actin cytoskeleton is triggered by the assembly of specific proteins inside cells in response to the specific recognition between adsorbed Fn molecules and integrin receptors located at the cell surface.[31,42,43] It is also worth noting that actin cables are formed in response to the recruitment of many ligand/integrin pairs at the cell surface and that many different protein adapters/signals are also involved inside cells [talin, paxillin, vinculin, focal adhesion kinase (FAK), sarcoma protein (Src), etc.] to ensure the development of normal cytoskeleton.[44] On the basis of our results, we can propose that the inhibition of cell adhesion and spreading obtained here might arise from three different reasons: (i) a masking by NPs of the cell-binding motif (RGD sequence) on Fn molecules, (ii) a physical masking of the surface by NPs strongly anchored via Fn molecules, and/or (iii) an insufficient mechanical attachment of NPs to the surface leading to weak cell adhesion. These hypotheses are summarized in the chart in Figure 7. First, the Fn layer is formed on surfaces before the incubation with NPs, and cells are finally seeded on surfaces (Figure 7A). The first assumption of molecular hindrance because of NPs adsorbed on cell recognition patterns of Fn can be disallowed by considering our ELISAs. Indeed, ELISA results showed that specific antibodies had no problem to access their binding sites on adsorbed Fn molecules. It is however important to remember that integrin receptors are inserted in the membrane of cells; therefore, they are closely surrounded with other molecules (lipids and proteins mainly) and are not freely diffusing in the medium, as antibodies can do under ELISA conditions. Therefore, even if ELISAs showed that there is probably no molecular hindrance because of NPs in the integrin/Fn recognition, we cannot exclude a limited access to Fn by integrins because these receptors are embedded within a supramolecular assembly of lipids and proteins (i.e., the cell membrane).

The second hypothesis suggests that cells could not access the surface because of the presence of numerous aggregates of NPs tightly bound to adsorbed Fn molecules (see Figure 7B). In fact, this hypothesis considers that the surface itself is masked and that aggregates of NPs generate a topography on the surface, so that only some cells can attach on the surface and cannot spread properly (Figure 7C). This hypothesis is partially disallowed if we compare ESEM images obtained at a high concentration of AN-NPs on Fn-coated surfaces without and with pre-osteoblasts (compare images E and F of Figure 4 to images C and D of Figure 1). Indeed, as seen on these images, the cells have redistributed the NPs on the surface, indicating that they can manage to access the surface by removing and redistributing some of the aggregates of surface-bound NPs.

In the last hypothesis, we suggest that cells have tried to adhere on NPs via specific interaction with integrins. This is

dx.doi.org/10.1021/la302219v | *Langmuir* 2012, 28, 13660−13667

conceivable if we consider that adsorbed Fn molecules are not frozen on the surface. Indeed, a protein adsorbed on a surface is always mobile and in equilibrium between a free and an adsorbed form.[18,19] Therefore, in our case, aggregates of NPs provide a competing surface to Fn molecules already adsorbed on Petri dishes. As a result, some Fn molecules might have desorbed from the surface of Petri dishes to adsorb on aggregates of NPs. Finally, the cells found two types of Fn on the surface: one type was directly bound to the Petri dish, and the other type was adsorbed on aggregates of NPs (Figure 7A′). One should notice that, in the early events of cell spreading, even before the stress fibers are formed, cells are able to develop large forces that are presumably associated with the actin cytoskeleton.[45,46] In the case of Fn-coated surfaces with NPs, cell integrins might have recognized Fn-coated aggregates of NPs. At this stage, cells might have tried to spread on the surface by exerting a mechanical stress on these anchoring points through the specific assembly of cytoskeleton elements in response to integrin−Fn recognition (Figure 7B′). Then, because of the weak attachment of NPs on the surface, cells might have grabbed Fn/NP aggregates from the surface. Such brutal tearing off of Fn-coated aggregates from the surface might have released the traction force of actin fibers very suddenly, which probably provoked their relaxation, as observed previously on live cells by dissecting their actin skeleton with laser nanoscissors.[47] The release of the traction force exerted by actin fibers upon detachment of Fn/NP aggregates from the surface might have pulled integrin−Fn/NP complexes on the cell body. As a result, the actin cytoarchitecture appeared disrupted with an aggregated structure, even on top of cells, in response to Fn/NP complexes still recognized by integrins (Figure 7C′).

4. CONCLUSION

In recent years, many efforts were made to assess the toxicity of NPs. In a recent report, the exposure of U.S. and U.K. populations to nanosized TiO_2 (in food and personal care products) was found to be as high as milligrams per kilogram of body weight and per day.[48] Some research groups remarkably demonstrated the crucial importance of taking into account the interaction of NPs with biomolecules for nanotoxicology. This approach aims at determining the toxicity under more realistic conditions and at identifying any unexpected side effects. Indeed, if some NPs are not found toxic because they do not reach the interior of cells, their association with biomolecules could completely change the deal by facilitating their cellular uptake. In light of our results, it is clear that, even without disturbing the specific recognition between integrins and Fn, TiO_2 NPs can greatly influence the cell behavior and structure on surfaces. These results highlight the ability of NPs to perturb cellular functions not only through a toxic mechanism but also by interacting with biomolecules from the extracellular matrix.

■ ASSOCIATED CONTENT

Supporting Information

Protocol and results of ELISAs using mono- and polyclonal antibodies that are specific for various regions of Fn (the whole protein and the RGD consensus sequence). This material is available free of charge via the Internet at http://pubs.acs.org.

■ AUTHOR INFORMATION

Corresponding Author

*Telephone: +33-3-44-23-73-56. Fax: +33-3-44-23-79-42. E-mail: kelkirat@utc.fr.

Author Contributions

†These authors contributed equally to this work.

Notes

The authors declare no competing financial interest.

■ ACKNOWLEDGMENTS

The financial support of the Centre National de la Recherche Scientifique (CNRS), of the French Ministry of Research and of the Université de Technologie de Compiègne (UTC, Plan de Pluriformation "Assemblages Biomimétiques, PPF BIO-MIM", Fondation-Programme Toxicologie-Eco Toxicologie Projet NP_LUNG) is gratefully acknowledged. The authors thank the Service d'Analyse Physico-Chimique (SAPC) of the UTC for providing ESEM and TEM facilities.

■ REFERENCES

(1) Lundqvist, M.; Stigler, J.; Elia, G.; Lynch, I.; Cedervall, T.; Dawson, K. A. Nanoparticle size and surface properties determine the protein corona with possible implications for biological impacts. *Proc. Natl. Acad. Sci. U.S.A.* **2008**, *105*, 14265−14270.

(2) Nel, A. E.; Madler, L.; Velegol, D.; Xia, T.; Hoek, E. M.; Somasundaran, P.; Klaessig, F.; Castranova, V.; Thompson, M. Understanding biophysicochemical interactions at the nano−bio interface. *Nat. Mater.* **2009**, *8*, 543−557.

(3) Lundqvist, M.; Sethson, I.; Jonsson, B. H. Protein adsorption onto silica nanoparticles: Conformational changes depend on the particles' curvature and the protein stability. *Langmuir* **2004**, *20*, 10639−10647.

(4) Tenuta, T.; Monopoli, M. P.; Kim, J.; Salvati, A.; Dawson, K. A.; Sandin, P.; Lynch, I. Elution of labile fluorescent dye from nanoparticles during biological use. *PLoS One* **2011**, *6*, No. e25556.

(5) Strehle, M. A.; Rosch, P.; Petry, R.; Hauck, A.; Thull, R.; Kiefer, W.; Popp, J. A Raman spectroscopic study of the adsorption of fibronectin and fibrinogen on titanium dioxide nanoparticles. *Phys. Chem. Chem. Phys.* **2004**, *6*, 5232−5236.

(6) Sund, J.; Alenius, H.; Vippola, M.; Savolainen, K.; Puustinen, A. Proteomic characterization of engineered nanomaterial−protein interactions in relation to surface reactivity. *ACS Nano* **2011**, *5*, 4300−4309.

(7) Allouni, Z. E.; Cimpan, M. R.; Hol, P. J.; Skodvin, T.; Gjerdet, N. R. Agglomeration and sedimentation of TiO_2 nanoparticles in cell culture medium. *Colloids Surf., B* **2009**, *68*, 83−87.

(8) Lynch, I.; Dawson, K. A. Protein−nanoparticle interactions. *Nano Today* **2008**, *3*, 40−47.

(9) Cedervall, T.; Lynch, I.; Foy, M.; Berggard, T.; Donnelly, S. C.; Cagney, G.; Linse, S.; Dawson, K. A. Detailed identification of plasma proteins adsorbed on copolymer nanoparticles. *Angew. Chem., Int. Ed. Engl.* **2007**, *46*, 5754−5756.

(10) Ji, Z.; Jin, X.; George, S.; Xia, T.; Meng, H.; Wang, X.; Suarez, E.; Zhang, H.; Hoek, E. M.; Godwin, H.; Nel, A. E.; Zink, J. I. Dispersion and stability optimization of TiO_2 nanoparticles in cell culture media. *Environ. Sci. Technol.* **2010**, *44*, 7309−7314.

(11) Kim, H.; Liu, X.; Kobayashi, T.; Kohyama, T.; Wen, F.-Q.; Romberger, D. J.; Conner, H.; Gilmour, P. S.; Donaldson, K.; MacNee, W.; Rennard, S. I. Ultrafine carbon black particles inhibit human lung fibroblast-mediated collagen gel contraction. *Am. J. Respir. Cell Mol. Biol.* **2003**, *28*, 111−121.

(12) Brown, D. M.; Wilson, M. R.; MacNee, W.; Stone, V.; Donaldson, K. Size-dependent proinflammatory effects of ultrafine polystyrene particles: A role for surface area and oxidative stress in the enhanced activity of ultrafines. *Toxicol. Appl. Pharmacol.* **2001**, *175*, 191−199.

(13) Brown, D. M.; Stone, V.; Findlay, P.; MacNee, W.; Donaldson, K. Increased inflammation and intracellular calcium caused by ultrafine carbon black is independent of transition metals or other soluble components. *Occup. Environ. Med.* **2000**, *57*, 685−691.
(14) Lynch, I.; Salvati, A.; Dawson, K. A. Protein−nanoparticle interactions: What does the cell see? *Nat. Nanotechnol.* **2009**, *4*, 546−547.
(15) Buzea, C.; Pacheco, I. I.; Robbie, K. Nanomaterials and nanoparticles: Sources and toxicity. *Biointerphases* **2007**, *2*, MR17−MR71.
(16) Maiorano, G.; Sabella, S.; Sorce, B.; Brunetti, V.; Malvindi, M. A.; Cingolani, R.; Pompa, P. P. Effects of cell culture media on the dynamic formation of protein−nanoparticle complexes and influence on the cellular response. *ACS Nano* **2010**, *4*, 7481−7491.
(17) Casals, E.; Pfaller, T.; Duschl, A.; Oostingh, G. J.; Puntes, V. Time evolution of the nanoparticle protein corona. *ACS Nano* **2010**, *4*, 3623−3632.
(18) Nonckreman, C. J.; Rouxhet, P. G.; Dupont-Gillain, C. C. Dual radiolabeling to study protein adsorption competition in relation with hemocompatibility. *J. Biomed. Mater. Res., Part A* **2007**, *81*, 791−802.
(19) Nonckreman, C. J.; Fleith, S.; Rouxhet, P. G.; Dupont-Gillain, C. C. Competitive adsorption of fibrinogen and albumin and blood platelet adhesion on surfaces modified with nanoparticles and/or PEO. *Colloids Surf., B* **2010**, *77*, 139−149.
(20) Ellingsen, J. E. A study on the mechanism of protein adsorption to TiO_2. *Biomaterials* **1991**, *12*, 593−596.
(21) Chothia, C.; Jones, E. Y. The molecular structure of cell adhesion molecules. *Annu. Rev. Biochem.* **1997**, *66*, 823−862.
(22) Effah, E. A.; Bianco, P. D.; Ducheyne, P. Crystal structure of the surface oxide layer on titanium and its changes arising from immersion. *J. Biomed. Mater. Res.* **1995**, *29*, 73−80.
(23) Margevicius, K. J.; Bauer, T. W.; McMahon, J. T.; Brown, S. A.; Merritt, K. Isolation and characterization of debris in membranes around total joint prostheses. *J. Bone Jt. Surg., Am. Vol.* **1994**, *76*, 1664−1675.
(24) Frisken, K. W.; Dandie, G. W.; Lugowski, S.; Jordan, G. A study of titanium release into body organs following the insertion of single threaded screw implants into the mandibles of sheep. *Aust. Dent. J.* **2002**, *47*, 214−217.
(25) Gerhardt, L.-C.; Jell, G.; Boccaccini, A. Titanium dioxide (TiO_2) nanoparticles filled poly(D,L lactid acid) (PDLLA) matrix composites for bone tissue engineering. *J. Mater. Sci.: Mater. Med.* **2007**, *18*, 1287−1298.
(26) Hashimoto, M.; Takadama, H.; Mizuno, M.; Kokubo, T. Mechanical properties and apatite forming ability of TiO_2 nanoparticles/high density polyethylene composite: Effect of filler content. *J. Mater. Sci. Mater. Med.* **2007**, *18*, 661−668.
(27) Tsuang, Y. H.; Sun, J. S.; Huang, Y. C.; Lu, C. H.; Chang, W. H.; Wang, C. C. Studies of photokilling of bacteria using titanium dioxide nanoparticles. *Artif. Organs* **2008**, *32*, 167−174.
(28) Ingham, E.; Fisher, J. Biological reactions to wear debris in total joint replacement. *Proc. Inst. Mech. Eng., Part H* **2000**, *214*, 21−37.
(29) Edwards, J.; Schulze, E.; Sabokbar, A.; Gordon-Andrews, H.; Jackson, D.; Athanasou, N. A. Absence of lymphatics at the bone−implant interface: Implications for periprosthetic osteolysis. *Acta Orthop.* **2008**, *79*, 289−294.
(30) Bernier, M. C.; El Kirat, K.; Besse, M.; Morandat, S.; Vayssade, M. Pre-osteoblasts and fibroblasts respond differently to anatase titanium dioxide nanoparticles: A cytotoxicity and inflammation study. *Colloids Surf., B* **2012**, *90*, 68−74.
(31) Frame, M.; Norman, J. A tal(in) of cell spreading. *Nat. Cell Biol.* **2008**, *10*, 1017−1019.
(32) Pankov, R.; Yamada, K. M. Fibronectin at a glance. *J. Cell Sci.* **2002**, *115*, 3861−3863.
(33) Moffat, J. R.; Sefiane, K.; Shanahan, M. E. Effect of TiO_2 nanoparticles on contact line stick-slip behavior of volatile drops. *J. Phys. Chem. B* **2009**, *113*, 8860−8866.
(34) Jemec, A.; Drobne, D.; Remskar, M.; Sepcic, K.; Tisler, T. Effects of ingested nano-sized titanium dioxide on terrestrial isopods (*Porcellio scaber*). *Environ. Toxicol. Chem.* **2008**, *27*, 1904−1914.
(35) Garcia, A. J.; Vega, M. D.; Boettiger, D. Modulation of cell proliferation and differentiation through substrate-dependent changes in fibronectin conformation. *Mol. Biol. Cell* **1999**, *10*, 785−798.
(36) Hashimoto, K.; Irie, H.; Fujishima, A. TiO_2 photocatalysis: A historical overview and future prospects. *Jpn. J. Appl. Phys.* **2005**, *44*, 8269−8285.
(37) Tsuji, J. S.; Maynard, A. D.; Howard, P. C.; James, J. T.; Lam, C.-W.; Warheit, D. B.; Santamaria, A. B. Research strategies for safety evaluation of nanomaterials, part IV: Risk assessment of nanoparticles. *Toxicol. Sci.* **2006**, *89*, 42−50.
(38) Furlong, D. N. Surface chemistry of silica coatings of titania. In *Colloidal Silica—Fundamentals and Applications*; Bergna, H. E., Roberts, W. O., Eds.; CRC Press (Taylor and Francis Group): Boca Raton, FL, 2005; Chapter 52, pp 689−699.
(39) Rapuano, B. E.; MacDonald, D. E. Surface oxide net charge of a titanium alloy: Modulation of fibronectin-activated attachment and spreading of osteogenic cells. *Colloids Surf., B* **2011**, *82*, 95−103.
(40) Lavenus, S.; Pilet, P.; Guicheux, J.; Weiss, P.; Louarn, G.; Layrolle, P. Behaviour of mesenchymal stem cells, fibroblasts and osteoblasts on smooth surfaces. *Acta Biomater.* **2011**, *7*, 1525−1534.
(41) Babiuch, K.; Becer, C. R.; Gottschaldt, M.; Delaney, J. T.; Weisser, J.; Beer, B.; Wyrwa, R.; Schnabelrauch, M.; Schubert, U. S. Adhesion of pre-osteoblasts and fibroblasts onto poly(pentafluorostyrene)-based glycopolymeric films and their biocompatibility. *Macromol. Biosci.* **2011**, *11*, 535−548.
(42) Dzamba, B. J.; Jakab, K. R.; Marsden, M.; Schwartz, M. A.; DeSimone, D. W. Cadherin adhesion, tissue tension, and noncanonical Wnt signaling regulate fibronectin matrix organization. *Dev. Cell* **2009**, *16*, 421−432.
(43) Chiquet, M.; Gelman, L.; Lutz, R.; Maier, S. From mechanotransduction to extracellular matrix gene expression in fibroblasts. *Biochim. Biophys. Acta* **2009**, *1793*, 911−920.
(44) Wierzbicka-Patynowski, I.; Schwarzbauer, J. E. The ins and outs of fibronectin matrix assembly. *J. Cell Sci.* **2003**, *116*, 3269−3276.
(45) Dubin-Thaler, B. J.; Hofman, J. M.; Cai, Y.; Xenias, H.; Spielman, I.; Shneidman, A. V.; David, L. A.; Dobereiner, H. G.; Wiggins, C. H.; Sheetz, M. P. Quantification of cell edge velocities and traction forces reveals distinct motility modules during cell spreading. *PLoS One* **2008**, *3*, No. e3735.
(46) Giannone, G.; Dubin-Thaler, B. J.; Dobereiner, H. G.; Kieffer, N.; Bresnick, A. R.; Sheetz, M. P. Periodic lamellipodial contractions correlate with rearward actin waves. *Cell* **2004**, *116*, 431−443.
(47) Kumar, S.; Maxwell, I. Z.; Heisterkamp, A.; Polte, T. R.; Lele, T. P.; Salanga, M.; Mazur, E.; Ingber, D. E. Viscoelastic retraction of single living stress fibers and its impact on cell shape, cytoskeletal organization, and extracellular matrix mechanics. *Biophys. J.* **2006**, *90*, 3762−3773.
(48) Weir, A.; Westerhoff, P.; Fabricius, L.; Hristovski, K.; von Goetz, N. Titanium dioxide nanoparticles in food and personal care products. *Environ. Sci. Technol.* **2012**, *46*, 2242−2250.